

Performance Improvement of YBCO Coil for High-Field HTS-SMES Based on Homogenized Distribution of Magnetically-Mechanically Influenced Critical Current

Kohei Higashikawa, Taketsune Nakamura, Michinaka Sugano, Koji Shikimachi, Naoki Hirano, and Shigeo Nagaya

Abstract—Generally speaking for a HTS coil, perpendicular magnetic field to conductor's broad surface should be suppressed as small as possible in relation to the magnetic anisotropy. This is a reason why toroidal coil with relatively many elementary coils is expected for HTS-SMES. On the other hand, from the point of view of the homogenization of critical current distribution in the coil, perpendicular field and parallel field should be balanced corresponding to the ratio of the magnetic anisotropy. This means that a certain level of the perpendicular field is effective to reduce local heat generation in the coil. Furthermore, this concept is especially reasonable for a high-field coil with usual winding method (flat-wise winding) because the perpendicular field does not induce hoop stress which decreases the critical current. In this paper, we show these findings through an optimal design of a MOCVD-YBCO toroidal coil for 2 GJ class SMES taking account of magnetically and mechanically influenced $J - E$ characteristics.

Index Terms—Hoop stress, mechanical strain, optimal design, SMES, YBCO coated conductor.

I. INTRODUCTION

IN JAPAN, the applicability of YBCO coated conductor to SMES has been explored under a national project by NEDO since FY2004. As a part of the project, we carried out a conceptual design of a high-field (over 10 T) YBCO coil at 20 K, and suggested that YBCO coated conductor could realize a very compact SMES magnet compared with a conventional one using Nb-Ti conductor [1]. Furthermore, it was also indicated that such a high-field coil could be realized not only by good transport characteristics of the YBCO material against magnetic field but also by high mechanical strength of Hastelloy substrate against hoop stress.

Manuscript received August 24, 2007. This work was supported by the New Energy and Industrial Technology Development Organization (NEDO), under the Research and Development of Superconducting Magnetic Energy Storage System sponsored by Agency of Natural Resources and Energy, Ministry of Economy, Trade and Industry (METI). In addition, YBCO coated conductors used in this work were produced by Chubu Electric Power Co., supported by NEDO through ISTEK, as the Collaborative Research and Development of Fundamental Technologies for Superconductivity Applications. The design method for HTS-SMES coil was developed with the support of Grant-in-Aid for JSPS Fellows (182788) by the Ministry of Education, Science, Sports and Culture in Japan.

K. Higashikawa, T. Nakamura, and M. Sugano are with the Department of Electrical Engineering, Graduate School of Engineering, Kyoto University, Kyoto 615-8510, Japan (e-mail: kohei@asl.kuee.kyoto-u.ac.jp; tk_naka@kuee.kyoto-u.ac.jp).

K. Shikimachi, N. Hirano, and S. Nagaya are with the Chubu Electric Power Company, Inc., Nagoya 459-8522, Japan.

Digital Object Identifier 10.1109/TASC.2008.921890

On the other hand, the transport characteristics of the conductor vary with applied tensile strain caused by such stress [2]–[5]. For example, the critical current of a MOCVD-YBCO coated conductor broadly decreases with the strain, although the strain dependence maintains reversibility up to very high stress (over 1 GPa) [5]. This indicates that locally large heat generation, which should be prevented especially for a conduction-cooled coil, will be generated in high-field region because the critical current in such a region is greatly decreased by the strain as well as by the field. Therefore, such mechanical properties should be taken into account in the design of a high-field coil with high hoop stress.

Given this factor, we have developed an optimal design method of a YBCO coil taking account of the mechanical properties in the conductor. The transport performance of the coil is calculated by means of finite element method [6], [7], and the configuration of the coil is optimized by genetic algorithm [8], [9]. By this method, we have carried out a conceptual design of a 2 GJ class SMES coil using a MOCVD-YBCO coated conductor, and discussed the influence of the mechanical properties on the optimal configuration.

II. DESIGN METHOD

A. $J-E$ Expressions

According to percolation transition model [10], current density, J , versus electric field, E , characteristics in HTS materials can be expressed by using the minimum value, J_{cm} , the half value of width, J_0 and a parameter representing the shape, m , of local critical current density distribution [11]–[14]:

$$J = \begin{cases} J_{cm} + \left(\frac{m+1}{\rho_{FF}} E J_0^m \right)^{\frac{1}{m+1}} & \text{for } J_{cm} \geq 0 \text{ Am}^{-2} \\ -|J_{cm}| + \left(\frac{m+1}{\rho_{FF}} E J_0^m + |J_{cm}|^{m+1} \right)^{\frac{1}{m+1}} & \text{for } J_{cm} < 0 \text{ Am}^{-2} \end{cases} \quad (1)$$

where ρ_{FF} is resistivity at uniform flux flow. For this model, the dependences of temperature, T , and magnetic field, B , can also be considered by the following scaling functions of pinning force density, $F_{pm} = J_{cm}B$ and $F_{pk} = (J_{cm} + J_0)B$ [13], [14]:

$$\frac{F_{pm}}{F_{pm,MAX}(T)} = \alpha \left(\frac{B}{B_p(T)} \right)^\beta \left(1 - \frac{B}{B_p(T)} \right)^\delta$$

$$\frac{F_{pk}}{F_{pk,MAX}(T)} = \alpha \left(\frac{B}{B_p(T)} \right)^\beta \left(1 - \frac{B}{B_p(T)} \right)^\delta \quad (2)$$

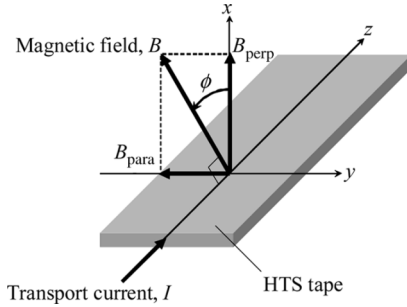


Fig. 1. Definition of the applied angle of magnetic field, ϕ .

where α , β and δ are pin parameters, and B_p is percolation transition magnetic field. It has been reported that (1), (2) can successfully describe $J - E$ characteristics of a YBCO coated conductor for wide ranges of temperature and magnetic field applied perpendicular to its broad surface [14]. Furthermore, in order to consider the dependence of applied angle of magnetic field, ϕ (see Fig. 1), we use equivalently perpendicular magnetic field, B_{eq} , as a substitute for B in (2) [15]:

$$B_{eq} = B \left(\cos^2 \phi + \frac{1}{\gamma^2} \sin^2 \phi \right)^{\frac{1}{2}} = \left(B_{perp}^2 + \left(\frac{1}{\gamma} B_{para} \right)^2 \right)^{\frac{1}{2}} \quad (3)$$

where B_{para} and B_{perp} are correspondingly parallel and perpendicular components of magnetic field (see Fig. 1), and γ is the anisotropic parameter [16]. The value of γ is 2.9 for a MOCVD-YBCO coated conductor assumed for the coil design. In addition, it has been reported that the scaling of the pinning force density holds also for applied tensile strain, ε [3]. Then, the strain dependence of $J - E$ characteristics can be predicted only by considering that of the maximum pinning force density, $F_{pm,MAX}$ and $F_{pk,MAX}$. We assume the following expressions.

$$F_{pm,MAX}(T, \varepsilon) = f(\varepsilon) F_{pm,MAX}(T, 0) \quad (4)$$

$$F_{pk,MAX}(T, \varepsilon) = f(\varepsilon) F_{pk,MAX}(T, 0) \quad (5)$$

$$f(\varepsilon) = A \left(1 - \left| \frac{\varepsilon - \varepsilon_{zero}}{\varepsilon_{lim} - \varepsilon_{zero}} \right|^\nu \right)$$

where ε_{zero} , ε_{lim} and ν are parameters, and A is calculated by $f(0) = 1$. Their values for the MOCVD-YBCO coated conductor are $\varepsilon_{zero} = 0.1\%$, $\varepsilon_{lim} = 1.6\%$, $\nu = 2.6$ for $F_{pm,MAX}$, and $\nu = 1.8$ for $F_{pk,MAX}$. By using (1)–(5), the strain dependence of critical current, I_c , determined with the electric field criterion, $E_c = 100 \mu V m^{-1}$, can be described very well at $T = 77.3$ K and self-field as shown in Fig. 2 [5]. Furthermore, (1)–(5) also give the already reported tendency [3], [4] that the strain dependence becomes more sensitive at higher temperature and/or higher magnetic field. We use (1)–(5) for the coil design.

B. Model

Toroidal configuration is expected for HTS-SMES coil from the point of view of conductor's consumption as well as stray magnetic field [17]. For this reason, toroidal configuration is selected for the coil design. Fig. 3 shows the design model for the toroidal coil. Each elementary coil is supposed to be fabricated by flat-wise winding method, and each turn of the coil is composed of insulator, the MOCVD-YBCO coated conductor and

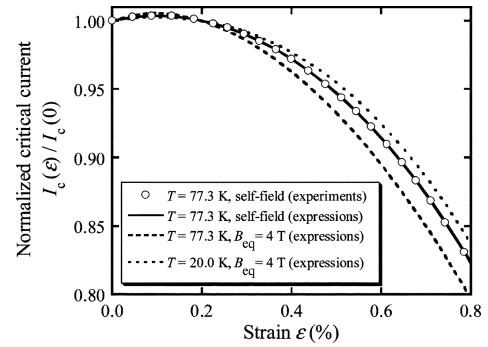


Fig. 2. Variation of critical current as a function of strain for the MOCVD-YBCO coated conductor. By (1)–(5), experimental data [5] is successfully described at 77.3 K and self-field, and the variation is predicted for other environment of temperature and magnetic field.

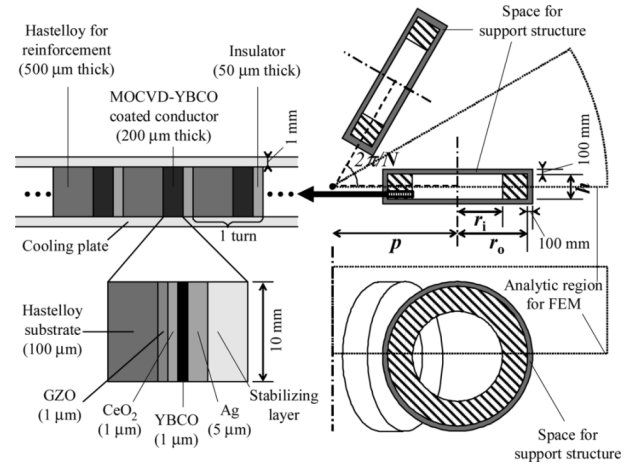


Fig. 3. Schematic diagram of the design model for toroidal coil.

Hastelloy tape for reinforcement. The conductor also includes Hastelloy as the substrate. The electromagnetic force induced in radial direction of each elementary coil (hoop force) is balanced only by the tensile force of the Hastelloy because both of its Young's modulus and cross-sectional area are much larger than those of other materials. Then, the tensile stress (hoop stress) applied to the Hastelloy, σ , is calculated by

$$\sigma = \frac{I}{wt} \times B_{para} \times r \quad (6)$$

where w , t and r are correspondingly the width, the thickness and the bend radius of the Hastelloy, and I is transport current to the conductor. Furthermore, we assure that the stress does not exceed the elastic limit of the Hastelloy in this design. Then the strain caused in the conductor is calculated by

$$\varepsilon = \frac{\sigma}{Y} \quad (7)$$

where Y is Young's modulus of the Hastelloy [18]. We investigate the influence of the hoop stress on the transport performance of the coil by considering (6), (7) into (1)–(5).

C. Conditions

The design is carried out for the minimization of the required length of the conductor. The design variables are the number, N , position, p , inside radius, r_i , outside radius, r_o and height, h , of

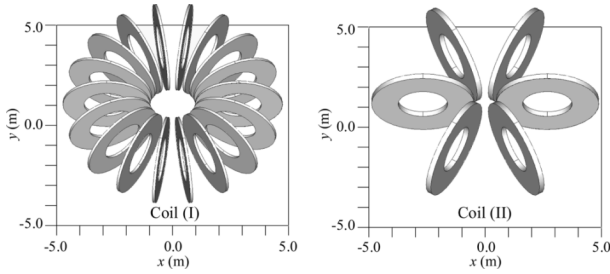


Fig. 4. Appearances of the designed coils. Coils (I) and (II) are the design results obtained without consideration and with consideration of the mechanical properties, respectively.

TABLE I
SPECIFICATIONS OF THE DESIGNED COILS

	Coil (I)	Coil (II)
Number of elementary coils, N	18	6
Position of elementary coil, p	2.85 m	2.68 m
Inside radius of elementary coil, r_i	0.97 m	1.07 m
Outside radius of elementary coil, r_o	1.88 m	2.20 m
Height of elementary coil, h	0.11 m	0.23 m
Required length of the conductor, l	1756 km	1772 km
Transport current, I	505 A	419 A
Minimum critical current, $I_{c, MIN}$	546 A (563 A)	477 A (486 A)
Maximum electric field, E_{MAX}	17.2 μVm^{-1} (8.4 μVm^{-1})	4.7 μVm^{-1} (3.1 μVm^{-1})
Flux flow loss, Q	195 W (99 W)	96 W (79 W)
Maximum hoop stress, σ_{MAX}	998 MPa	961 MPa
Maximum parallel magnetic field, $B_{para, MAX}$	12.0 T	12.7 T
Maximum perpendicular magnetic field, $B_{perp, MAX}$	2.9 T	5.1 T

Coils (I) and (II) are the design results obtained without consideration and with consideration of the mechanical properties, respectively. The values in parentheses are calculated without consideration of the mechanical properties.

the elementary coils, and their definitions are shown in Fig. 3. The optimal set of them is searched by genetic algorithm under the following constraint conditions.

- Operating temperature is 20 K.
- Stored energy is 2 GJ.
- Maximum electric field, E_{MAX} , does not exceed $E_c = 100 \mu\text{Vm}^{-1}$. This means that transport current is not larger than critical current everywhere in the coil.
- Total flux flow loss, Q , does not exceed 100 W.
- Maximum hoop stress, σ_{MAX} , does not exceed 1 GPa. The corresponding strain caused in the conductor is 0.47%. It has already been found that the conductor can reversibly tolerate such a strain in terms of $I_c - \varepsilon$ characteristics as well as mechanical strength [5].
- The number of unit coils is multiples of 3. The lower and the upper limits are set to be 6 and 63, respectively.

III. RESULTS AND DISCUSSION

We compare the design results between the case without consideration of the mechanical property (hereinafter called “Coil (I)”) and the case with consideration of that (hereinafter called “Coil (II)”). In other words, Coil (I) is designed under $f(\varepsilon) = 1$ for (4), and Coil (II) is obtained with consideration of (5) for (4). Fig. 4 shows the appearances of Coils (I) and (II), and Table I lists their specifications. Furthermore, Fig. 5 shows the distributions of magnetic field, hoop stress, critical current and electric field in an elementary coil for them.

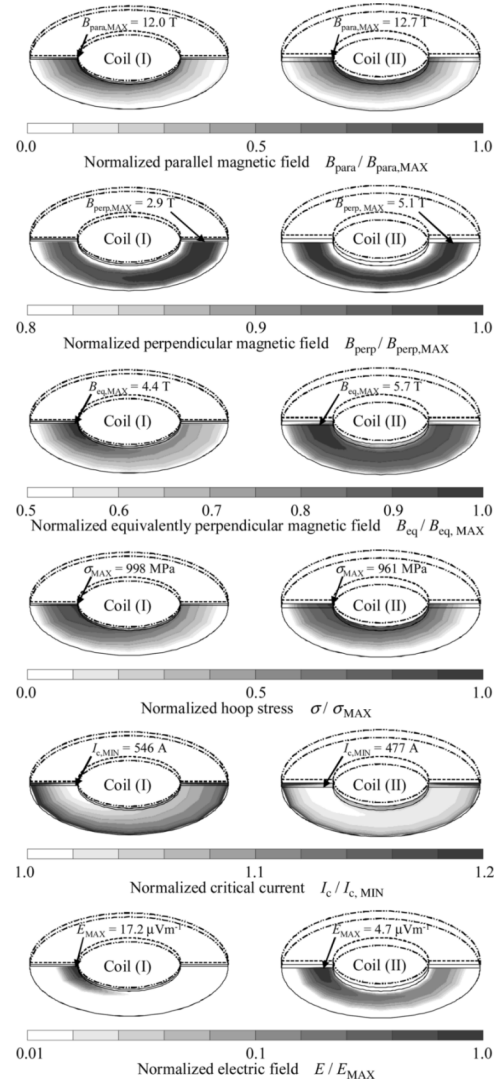


Fig. 5. Distributions of magnetic field, hoop stress, critical current and electric field in an elementary coil of the toroidal coil. Coils (I) and (II) are the design results obtained without consideration and with consideration of the mechanical properties, respectively.

Coil (I) has relatively many elementary coils, and then perpendicular magnetic field is well suppressed, e.g., 2.9 T for its maximum value, $B_{perp, MAX}$, with respect to 12.0 T for the maximum parallel magnetic field, $B_{para, MAX}$. This is a key reason why the toroidal configuration with relatively many elementary coils is expected for HTS-SMES. However, it should be noted that the transport performance of Coil (I) is greatly influenced by the mechanical properties. For example, E_{MAX} as well as Q becomes approximately 2 times as large as the case without consideration of the mechanical properties, and then Q largely exceeds the upper limit of 100 W. This strongly indicates the significance of the mechanical properties on the transport performance of the coil and the necessity of consideration of that for the design.

On the other hand, we obtain Coil (II) with consideration of the mechanical properties. It can be seen that the configuration of Coil (II) is quite different from that of Coil (I). In association with such a difference in the number of elementary coils, Coil (II) needs less transport current, I , to store the same energy because larger inductance is obtained with smaller number of the

elementary coils [9], e.g., $I = 419$ A for Coil (II) with respect to $I = 505$ A for Coil (I). However, it should be noted that perpendicular field of Coil (II) becomes much larger than that of Coil (I) instead, e.g., $B_{\text{perp,MAX}} = 5.1$ T for Coil (II) with respect to $B_{\text{perp,MAX}} = 2.9$ T for Coil (I). Surprisingly, this turns out to be the reason why Coil (II) becomes the optimal configuration by considering the mechanical properties.

For Coil (I), as stated above, perpendicular field is much smaller than parallel field. Then, as shown in Fig. 5, the distribution of B_{eq} , which almost dominates that of I_c , becomes similar to that of B_{para} . It should also be noted that the distribution of σ also corresponds to that of B_{para} because only the parallel field induces the hoop stress as expressed in (6). This means that critical current largely decreased by magnetic field is additionally degraded by high hoop stress, because the region of high B_{eq} is unfortunately and entirely exposed to high σ . This causes the great increase of E_{MAX} and Q . For Coil (II), on the other hand, perpendicular field is relatively large. Then, the distribution of B_{eq} is similar to that of B_{perp} . However, the perpendicular field does not induce the hoop stress. This brings about the situation that the region of high B_{eq} and that of high σ are separated from each other. For example, the maximum value of B_{eq} , $B_{\text{eq,MAX}}$, is located away from σ_{MAX} , while they are located almost at the same position for Coil (I). As a result, the decrement of the minimum critical current, $I_{c,\text{MIN}}$, due to the mechanical properties can be suppressed to 1.9% (from 486 A to 477 A) with respect to 3.0% (from 563 A to 546 A) for Coil (I). Then, the corresponding increment of Q is only 25% (from 79 W to 99 W) with respect to 97% (from 99 W to 195 W) for Coil (I). This is the reason why Coil (II) with high perpendicular field becomes the optimal configuration.

Furthermore, as shown in Fig. 5, it can also be found that the distribution of B_{eq} is homogenized for Coil (II) compared to the case with Coil (I). This is attributed to the fact that parallel field and perpendicular field are balanced according to the parameter of the magnetic anisotropy (see (3)). For example, $B_{\text{para,MAX}}/B_{\text{perp,MAX}} = 2.5$ for Coil (II) is close in value to $\gamma = 2.9$ compared with $B_{\text{para,MAX}}/B_{\text{perp,MAX}} = 4.1$ for Coil (I). Therefore, a certain value of perpendicular field is necessary to homogenize the distribution of B_{eq} . It should be noted that the homogenized distribution of B_{eq} leads that of I_c . As a result, the distribution of E is also homogenized, and then high electric field area is very large for Coil (II) compared to the case with Coil (I). This indicates that the heat generation in the coil can be shared by large area, and then the corresponding local heat generation can be suppressed. In fact, E_{MAX} for Coil (II) is much smaller than that for Coil (I).

From these results, it can be concluded that a certain level of perpendicular field is effective to homogenize critical current distribution in the coil, and this also leads the suppression of the increment of the heat generation caused by the hoop stress.

IV. CONCLUSION

We carried out an optimal design of a MOCVD-YBCO toroidal coil for 2 GJ class SMES taking account of magnetically and mechanically influenced $J - E$ characteristics. As a result, it was found that a certain level of perpendicular magnetic field to the conductor was effective to homogenize

the critical current distribution in the coil. Furthermore, such a perpendicular field could greatly suppress the increment of the heat generation caused by the hoop stress.

REFERENCES

- [1] K. Higashikawa, T. Nakamura, K. Shikimachi, N. Hirano, S. Nagaya, T. Kiss, and M. Inoue, "Conceptual design of HTS coil for SMES using YBCO coated conductor," *IEEE Trans. Appl. Supercond.*, vol. 17, no. 2, pp. 1990–1993, 2007.
- [2] N. Cheggour, J. W. Ekin, C. L. H. Thieme, Y.-Y. Xie, V. Selvamanickam, and R. Feenstra, "Reversible axial-strain effect in Y-Ba-Cu-O coated conductors," *Supercond. Sci. Technol.*, vol. 18, pp. S319–S324, 2005.
- [3] N. Cheggour, J. W. Ekin, and C. L. H. Thieme, "Magnetic-field dependence of the reversible axial-strain effect in Y-Ba-Cu-O coated conductors," *IEEE Trans. Appl. Supercond.*, vol. 15, no. 2, pp. 3577–3560, 2005.
- [4] D. Uglietti, B. Seeber, V. Abächerli, W. L. Carter, and R. Flükiger, "Critical currents versus applied strain for industrial Y-123 coated conductors at various temperatures and magnetic fields up to 19 T," *Supercond. Sci. Technol.*, vol. 19, pp. 869–872, 2006.
- [5] M. Sugano, T. Nakamura, K. Shikimachi, N. Hirano, and S. Nagaya, "Stress tolerance and fracture mechanism of solder joint of YBCO coated conductor," *IEEE Trans. Appl. Supercond.*, vol. 17, no. 2, pp. 3067–3070, 2007.
- [6] K. Higashikawa, T. Nakamura, and T. Hoshino, "Anisotropic distributions of current density and electric field in Bi-2223/Ag coil with consideration of multifilamentary structure," *Physica C*, vol. 419, pp. 129–140, 2005.
- [7] K. Higashikawa, T. Nakamura, and H. Okamoto, "Analysis of discharging characteristics in a Bi-2223/Ag coil for SMES with consideration of cooling capacity of a cryocooler," *IEEE Trans. Appl. Supercond.*, vol. 16, no. 2, pp. 578–581, 2006.
- [8] K. Higashikawa, T. Nakamura, T. Hoshino, and I. Muta, "Design of Bi-2223/Ag coil based on genetic algorithm and finite element method," *IEEE Trans. Appl. Supercond.*, vol. 15, no. 2, pp. 1895–1898, 2005.
- [9] K. Higashikawa, T. Nakamura, and H. Okamoto, "Optimal design of a Bi-2223/Ag coil for superconducting magnetic energy storage at different operating temperatures," *Supercond. Sci. Technol.*, vol. 18, pp. 1445–1453, 2005.
- [10] K. Yamafuji and T. Kiss, "Current-voltage characteristics near the glass-liquid transition in high- T_c superconductors," *Physica C*, vol. 213, pp. 9–22, 1997.
- [11] T. Kiss, T. Nakamura, N. Mishiro, and K. Hasegawa, M. Inoue, M. Takeo, F. Irie, and K. Yamafuji, "Transport characteristics in high T_c superconductors," in *Proc. MT15*, 1998, no. 2, pp. 1052–1055.
- [12] T. Kiss, K. Hasegawa, M. Inoue, M. Takeo, H. Okamoto, and F. Irie, "Critical current properties in high T_c superconductors," (in Japanese) *Cryogenic Engineering (Teion-Kogaku)*, vol. 34, no. 7, pp. 322–331, 1999.
- [13] T. Kiss, M. Inoue, T. Kuga, M. Ishimaru, S. Egashira, S. Irie, T. Ohta, K. Imamura, M. Yasunaga, M. Takeo, T. Matsushita, Y. Iijima, K. Kakimoto, T. Saitoh, S. Awaji, K. Watanabe, and Y. Shiohara, "Critical current properties in HTS tapes," *Physica C*, vol. 392–396, pp. 1053–1062, 2003.
- [14] M. Inoue, T. Kiss, T. Kuga, M. Ishimaru, M. Takeo, T. Matsushita, Y. Iijima, K. Kakimoto, T. Saitoh, S. Awaji, K. Watanabe, and Y. Shiohara, "Critical current properties of a YBCO coated conductor in high magnetic fields," (in Japanese) *IEEJ Trans. Fundamentals and Materials*, vol. 123, no. 6, pp. 593–599, 2003.
- [15] T. Nakamura, S. Tsuchiya, A. Fujio, T. Hoshino, and I. Muta, "Angular dependence of E-J characteristics and dissipative properties in Bi-2223/Ag tape," *Supercond. Sci. Technol.*, vol. 15, pp. 230–235, 2002.
- [16] T. Nakamura, T. Yamamoto, S. Tsuchiya, A. Fujio, T. Hoshino, I. Muta, S. S. Oh, and H. S. Ha, "Anisotropy of critical current and glass-liquid transition flux density in Bi-2223/Ag tape," *Supercond. Sci. Technol.*, vol. 13, pp. 1521–1525, 2000.
- [17] S. Noguchi, A. Ishiyama, A. Akita, H. Kasahara, Y. Tatsuta, and S. Kouso, "An optimal configuration design method for HTS-SMES coils," *IEEE Trans. Appl. Supercond.*, vol. 15, no. 2, pp. 1927–1930, 2005.
- [18] C. C. Clickner, J. W. Ekin, N. Cheggour, C. L. H. Thieme, Y. Qiao, Y.-Y. Xie, and A. Goyal, "Mechanical properties of pure Ni and Ni-alloy substrate materials for Y-Ba-Cu-O coated superconductors," *Cryogenics*, vol. 46, pp. 432–438, 2006.